Max-Planck-Institut
für Mathematik
in den Naturwissenschaften
Leipzig

Examples of nonlinear homogenization in plane strain involving degenerate energies

by

Isaac Chenchiah and Kaushik Bhattacharya

Preprint no.: 49 2004

Examples of nonlinear homogenization in plane strain involving degenerate energies

By Isaac V. Chenchiah[1] and Kaushik Bhattacharya[2]

[1]*Max Planck Institute for Mathematics in the Sciences, Inselstr. 22, D-04103 Leipzig, Germany (Isaac.Chenchiah@mis.mpg.de)*
[2]*Division of Engineering and Applied Science, California Institute of Technology, Pasadena, CA 91125, USA (bhatta@caltech.edu)*

The study of polycrystals of shape-memory alloys and rigid-perfectly plastic materials gives rise to problems of nonlinear homogenization involving degenerate energies. This paper presents a characterization of the stress and strain fields in a class of problems in plane strain, and uses it to study examples including checkerboards and hexagonal microstructures. Consequences for shape-memory alloys and rigid-perfectly plastic materials are discussed.

Keywords: homogenization; shape-memory polycrystals; rigid-perfect plasticity; localization; checkerboard microstructure

1. Introduction

This paper discusses model problems that provide insight into the nature of stress and strain fields in polycrystals made of shape-memory alloys. Our results also have relevance to the dual problem of plastic yielding of polycrystalline media.

Shape-memory behavior is the ability of certain materials to recover, on heating, apparently plastic deformations sustained below a critical temperature. In such materials, one has multiple stress-free states or variants, and they may co-exist in coherent fine-scale mixtures or microstructures. The origin of the shape-memory effect lies in the fact that the material can be deformed by coherently changing the microstructure through a rearrangement of the variants. Thus, the amount of strain recoverable by a single crystal in the shape-memory effect can be determined from crystallography (i.e., the number and stress-free strains of the variants).

The situation is more complex in polycrystals. Here the material is an assemblage of grains, each composed of the same material but with a different orientation, that are bonded together. The deformation of a grain through rearrangement of variants depends on its orientation and thus each grain may seek to deform differently. But the grains are bonded together, and thus constrain each other. Therefore an imposed strain is recoverable in a polycrystal if and only if the different grains can collectively and cooperatively adjust their microstructure to accommodate it. Interestingly, the amount of recoverable strain in a polycrystal can vary dramatically even amongst materials that have comparable recoverable strain as single crystals. Therefore, understanding the shape-memory effect in a polycrystal has received much attention. We refer the reader to Bhattacharya (2003) for a comprehensive discussion and references.

In this paper, we study model problems in the two-dimensional setting of plane infinitesimal strains corresponding to a two-variant material (square to rectangle transformation). The recoverable strains of a single crystal are confined to one (strain) direction, and the issue of interest is whether the polycrystal has any recoverable strains at all. This problem is motivated by an important class of materials that undergo the cubic to tetragonal transformation. We restrict the deformation of each grain to only those allowed by the formation and manipulation of microstructure (see DeSimone & James (2002) for a discussion of this assumption). So each grain is a locking material (Prager, 1957; Demengel & Suquet, 1986).

We provide an alternative proof to a result of Bhattacharya & Kohn (1997) that polycrystals of the two-variant material that possess sufficient symmetry are rigid, i.e., have no recoverable strains. Our main tool in obtaining this result is a characterization of the stress and strain fields in polycrystals of such materials: specifically we show that they satisfy hyperbolic partial differential equations. The strain (stress) is confined to lie on a certain one-dimensional line (two-dimensional plane) and this along with compatibility (equilibrium) gives the hyperbolic equations. However, the set changes from grain to grain, and thus the characteristics of our hyperbolic equations change orientation from grain to grain.

We also use this characterization to study in detail a series of examples of polycrystals. These examples demonstrate the result that polycrystals of the two-variant material that possess sufficient symmetry are rigid. They also demonstrate the hyperbolic nature of the strain and stress fields: First, the set of recoverable strains can be very sensitive to the orientation and arrangement of grains. Second, stress can localize along lines that propagate through the grains. Heuristically, consider a polycrystal subjected to an increasing macroscopic strain. Initially this strain may be accommodated uniformly by every grain, but gradually the poorly oriented grains begin to "lock", i.e., have accommodated all the strains that they could accomodate. The imposed strain now has to be accommodated by an inhomogeneous strain field that circumvents the locked grains till one has a network of fully locked grain. At this point, the stress is borne by the network of locked grains, and therefore the stress fields can become highly localized. This idea is made precise by the hyperbolic characterization. We note that the problem of localization of stress fields has also recently been studied numerically by Bhattacharya & Suquet (2004) in the setting of antiplane shear for realistic micro-geometries of grains.

The dual of the shape-memory problem discussed above concerns rigid-perfectly plastic materials. In this setting, if the single crystal of a material has a deficient number of slip systems, an important question is whether a polycrystal of this materials is macroscopically rigid-perfectly plastic or simply rigid. This issue is of interest in hexagonal materials (see Kochs *et al.* (1998) for a comprehensive discussion and references). It was recently formulated in a setting dual to ours by Kohn & Little (1998). Our ideas and results have implications for these problems.

Problems related to both the shape-memory effect and plasticity have been studied extensively recently using examples (Bhattacharya & Kohn, 1997; Kohn & Little, 1998; Bhattacharya *et al.*, 1999; Goldsztein, 2001, 2003; Garroni & Kohn, 2003). However, these have been confined to scalar problems. We find nontrivial differences in our current setting of plane strain.

Finally, our characterization of stress and strain fields is reminiscent of the classical theory of plastic slip-line fields (see, for example, Hill (1950)). This is

derived under the assumption of plane strain, isotropy and rigid-plasticity: that the stress in the plastic zone is confined to lie on a two-dimensional manifold (the yield-surface) and also satisfy equilibrium implies that it satisfies a hyperbolic equations. Similarly, our methods are reminiscent of classical plastic limit analysis (see, for example, Drucker *et al.* (1952)). These methods have been extensively used to study problems in isotropic homogeneous plasticity, and occasionally in isotropic heterogeneous media (see Drucker (1966) for an insightful discussion). However, we are unaware of the use of these ideas in anisotropic heterogeneous media.

2. Mathematical Formulation

We consider in two-dimensions a material with two variants that have transformation or stress-free strains $\pm \left(\begin{smallmatrix} 1 & 0 \\ 0 & -1 \end{smallmatrix}\right)$. These strains are compatible in the sense that one arrange them in a coherent microstructure. By making such microstructures, a single crystal of this material can attain average strains in the set

$$\widehat{\mathcal{S}} = \left\{ s \left(\begin{smallmatrix} 1 & 0 \\ 0 & -1 \end{smallmatrix}\right) \mid s \in \mathbb{R},\ |s| \leq 1 \right\}. \tag{2.1}$$

For a grain oriented at an angle θ, the corresponding set is given by

$$\widehat{\mathcal{S}}_\theta = \left\{ s\ \hat{\epsilon}_{2\theta} \mid s \in \mathbb{R},\ |s| \leq \sqrt{2} \right\} \tag{2.2}$$

where

$$\hat{\epsilon}_{2\theta} = \frac{1}{\sqrt{2}} \left(\begin{smallmatrix} \cos 2\theta & \sin 2\theta \\ \sin 2\theta & -\cos 2\theta \end{smallmatrix}\right).$$

The material considered here is called 'Two-Dimensional Diagonal Trace-Free Elastic Material' in Bhattacharya & Kohn (1997).

We assume that the energy density of a single crystal of this material is

$$\widehat{W}(\epsilon) := \begin{cases} 0 & \epsilon \in \widehat{\mathcal{S}} \\ \infty & \text{otherwise.} \end{cases}$$

Notice that we have assumed that the elastic moduli of each phase is infinite and thus may regard it as a locking material (Prager, 1957; Demengel & Suquet, 1986).

Let $R\colon \Omega \to SO(2)$ describe the texture of the polycrystal: $R(x)$ gives the orientation of a grain at x relative to the laboratory frame. We assume in what follows that R is piecewise constant. The effective energy density of a polycrystal with texture R is given by

$$\overline{W}(\bar{\epsilon}) := \inf_{\substack{\epsilon \in \mathcal{U}_{\text{ad}} \\ \langle \epsilon(x) \rangle = \bar{\epsilon}}} \fint_\Omega \widehat{W}(R^T(x)\epsilon(x)R(x))\ \mathrm{d}x$$

where

$$\mathcal{U}_{\text{ad}} := \left\{ u \in L^\infty(\Omega, \mathbb{R}^2) \mid \epsilon(u) \in L^\infty_{\text{per}}(\Omega, M^{2\times 2}_{\text{sym}}) \right\}.$$

It is easy to see that $\overline{W}$ is of the form

$$\overline{W}(\bar{\epsilon}) := \begin{cases} 0 & \bar{\epsilon} \in \overline{\mathcal{S}} \\ \infty & \text{otherwise} \end{cases}$$

where $\overline{\mathcal{S}}$ is the set of recoverable strains of the polycrystal; for a discussion see Chenchiah (2004). Chenchiah (2004), extending methods of Demengel & Suquet (1986), has also shown that $\overline{W}$ has the dual variational characterization,

$$\overline{W}(\bar{\epsilon}) := \sup_{\sigma \in \mathcal{S}_{\text{ad}}} \fint_\Omega \sigma \cdot \bar{\epsilon} - \widehat{W}^\star(R^T(x)\sigma(x)R(x)) \, \mathrm{d}x. \tag{2.3}$$

Here

$$\mathcal{S}_{\text{ad}} := \left\{ \sigma \in M^1_{\text{per}}(\Omega, M^{2\times 2}_{\text{sym}}) \mid \text{div}(\sigma) = 0 \right\},$$

$\mathcal{M}^1_{\text{per}}(\Omega, M^{2\times 2}_{\text{sym}})$, the dual of $L^\infty_{\text{per}}(\Omega, M^{2\times 2}_{\text{sym}})$, is the space of all periodic signed Radon measures with finite mass; $\text{div}(\sigma) = 0$ means

$$\int_\Omega \sigma \cdot \nabla\phi \, \mathrm{d}v = 0, \qquad \forall \phi \in \mathcal{C}^\infty_0(\Omega, \mathbb{R}^2);$$

and $\widehat{W}^\star$, the conjugate energy, is the Legendre dual of $\widehat{W}$:

$$\widehat{W}^\star(\sigma) = \max_\epsilon \Big(\sigma \cdot \epsilon - \widehat{W}(\epsilon) \Big) = \max_{\epsilon \in \widehat{\mathcal{S}}} \sigma \cdot \epsilon.$$

Specifically for grain oriented at an angle θ and the set $\widehat{\mathcal{S}}_\theta$ in (2.2), we have

$$\widehat{W}^\star_\theta(\sigma) = \widehat{W}^\star(R^T(x)\sigma(x)R(x)) = \sqrt{2} \, |\sigma \cdot \hat{\epsilon}_{2\theta}|. \tag{2.4}$$

We note some properties that the set of recoverable strains of a polycrystal inherits from the set of recoverable strains of a single crystal. $\widehat{\mathcal{S}}$ is convex, balanced (i.e., $\epsilon \in \widehat{\mathcal{S}} \implies -\epsilon \in \widehat{\mathcal{S}}$), has square symmetry (i.e., $\epsilon \in \widehat{\mathcal{S}} \implies R^T_{\frac{\pi}{2}} \epsilon R_{\frac{\pi}{2}} \in \widehat{\mathcal{S}}$) and contained in the subspace of trace-free matrices. It is easy to show that $\overline{\mathcal{S}}$ possesses the same properties. Further $0 \in \overline{\mathcal{S}}$. We shall call a polycrystal *rigid* if $\overline{\mathcal{S}} = \{0\}$ and *flexible* otherwise. A key issue in this paper is trying to understand whether a polycrystal of a two-variant material is rigid.

Finally, we discuss stress-fields concentrated on lines since they will play an important role in our examples. A divergence-free stress-field concentrated on a line with tangent $\hat{t}$ may be visualized as an element of a truss of structural mechanics that carries a certain force f parallel to itself. Alternately, it may be visualized by considering a piecewise constant stress field that is zero outside a strip of width τ along the line and equal to $\frac{f}{\tau}\hat{t} \otimes \hat{t}$ on it and then letting $\tau \to 0$. The total force it contributes to a surface it intersects transversely is $f\text{sign}(\hat{n} \cdot \hat{t})\hat{t}$ where $\hat{n}$ is the outward normal to the surface. It's average over a region $\mathcal{D}$ is given as

$$\langle \sigma \rangle_{\mathcal{D}} = \frac{\text{length of the line in } \mathcal{D}}{\text{area of } \mathcal{D}} f\hat{t} \otimes \hat{t}.$$

We call f the force of the stress field concentrated on the line and $f\hat{t} \otimes \hat{t}$ the value of the stress field. The stress is tensile if $f > 0$ and compressive otherwise. Finally, if n lines, with force f_i concentrated on the i^{th} line, intersect at a point, then this stress field is divergence free precisely when $\sum_{i=1}^n f_i \hat{t}_i = 0$, where $\hat{t}_i$ is the tangent to the ith line directed away from the point.

3. Strain and stress fields

(*a*) *Single crystals*

Consider any zero-energy strain field in a single crystal oriented at an angle θ. From (2.2) such a strain field is constrained to be of the form

$$\epsilon(x,y) = s(x,y)\hat{\epsilon}_{2\theta}, \qquad |s(x,y)| \leqslant \sqrt{2}$$

for some $s \in L^\infty(\mathbb{R}^2, \mathbb{R})$. It also satisfies the strain compatibility equation,

$$\frac{\partial^2}{\partial y^2}\epsilon_{xx} - 2\frac{\partial^2}{\partial x \partial y}\epsilon_{xy}, + \frac{\partial^2}{\partial x^2}\epsilon_{yy} = 0.$$

Together, they imply that s satisfies the hyperbolic partial differential equation

$$\Box_\theta^2 \; s(x,y) = 0,$$

where

$$\Box_\theta^2 \equiv \cos 2\theta \frac{\partial^2}{\partial x^2} + 2\sin 2\theta \frac{\partial^2}{\partial x \; \partial y} - \cos 2\theta \frac{\partial^2}{\partial y^2}.$$

Since ϵ is allowed to be discontinuous (in L^∞), we interpret these equations in the sense of distributions. Notice that $\Box_\theta^2$ is the wave operator with the 'space-time' coordinates oriented at an angle θ to the $x-y$ coordinates. The characteristics of the above wave equation are inclined at angles $\theta - \frac{\pi}{4}$ and $\theta + \frac{\pi}{4}$ respectively.

Let H be the displacement gradient. The constraint $\epsilon \in \widehat{\mathcal{S}}_\theta$ is equivalent to the constraint $H \in \widehat{\mathcal{S}}_\theta \oplus \text{Span}\left\{ \left(\begin{smallmatrix} 0 & 1 \\ -1 & 0 \end{smallmatrix}\right) \right\}$:

$$H(x,y) = s(x,y)\hat{\epsilon}_{2\theta} + \omega(x,y)\frac{1}{\sqrt{2}}\left(\begin{smallmatrix} 0 & 1 \\ -1 & 0 \end{smallmatrix}\right), \qquad |s(x,y)| \leqslant \sqrt{2} \tag{3.1}$$

for some $s \in L^\infty(\mathbb{R}^2, \mathbb{R})$ and some $\omega \colon \mathbb{R}^2 \to \mathbb{R}$. This with the compatibility condition $\nabla \times H = 0$ implies the non-homogeneous transport equation,

$$\nabla w(x,y) = \left(\begin{smallmatrix} -\sin 2\theta & \cos 2\theta \\ \cos 2\theta & \sin 2\theta \end{smallmatrix}\right) \nabla s(x,y) \tag{3.2}$$

and thus the hyperbolic partial differential equation,

$$\Box_\theta^2 \; w(x,y) = 0.$$

From these results, it is easy to show (see Chenchiah (2004) for details) that the displacement gradient in a grain oriented at an angle θ has the form

$$\begin{aligned} H(x,y) = {} & p(\cos(\theta + \frac{\pi}{4})x + \sin(\theta + \frac{\pi}{4})y) \; \hat{n}(\theta - \frac{\pi}{4}) \otimes \hat{n}(\theta + \frac{\pi}{4}) \\ & + q(\cos(\theta - \frac{\pi}{4})x + \sin(\theta - \frac{\pi}{4})y) \; \hat{n}(\theta + \frac{\pi}{4}) \otimes \hat{n}(\theta - \frac{\pi}{4}) + c\left(\begin{smallmatrix} 0 & 1 \\ -1 & 0 \end{smallmatrix}\right). \end{aligned}$$

Here $p, q \in L^\infty$, $c \in \mathbb{R}$ is a constant and $\hat{n}(\cdot) = \begin{pmatrix} \cos(\cdot) \\ \sin(\cdot) \end{pmatrix}$. In words, the displacement gradient field in a grain oriented at θ is the superposition of the displacement gradient supported on the characteristics in that grain. Further, the characteristic

oriented at $\theta - \frac{\pi}{4}$ supports a constant displacement gradient which is parallel to $\hat{n}(\theta - \frac{\pi}{4}) \otimes \hat{n}(\theta + \frac{\pi}{4})$ and the characteristic oriented at $\theta + \frac{\pi}{4}$ supports a constant displacement gradient which is parallel to $\hat{n}(\theta + \frac{\pi}{4}) \otimes \hat{n}(\theta - \frac{\pi}{4})$.

We now turn to the stress fields that have zero conjugate energy. From (2.4), $\widehat{W}^\star_\theta(\sigma) = 0$ precisely when $\sigma \cdot \hat{\epsilon}_{2\theta} = 0$. This occurs precisely when σ is of the form

$$\sigma(x,y) = \sigma_h(x,y)I + \sqrt{2}t(x,y)\hat{\epsilon}_{2\theta+\frac{\pi}{2}}$$

where $I \equiv \left(\begin{smallmatrix} 1 & 0 \\ 0 & 1 \end{smallmatrix}\right)$. This with the equilibrium equation $\mathrm{div}(\sigma) = 0$ implies the non-homogeneous transport equation

$$\nabla\sigma_h(x,y) = \left(\begin{smallmatrix} -\sin 2\theta & \cos 2\theta \\ \cos 2\theta & \sin 2\theta \end{smallmatrix}\right) \nabla t(x,y).$$

This implies that $\Box^2_\theta\ t(x,y) = 0$ and $\Box^2_\theta\ \sigma_h(x,y) = 0$.

(*b*) *Polycrystals*

The displacement gradient and stress fields must satisfy the relations above in each grain. In addition, the displacement gradient has to be compatible across the grain boundary and the stress equilibriated. Therefore the jump in displacement gradient and stress satisfy

$$[\![H]\!] \parallel \hat{n}^\perp \otimes \hat{n}, \quad [\![\sigma]\!] \parallel \hat{n}^\perp \otimes \hat{n}^\perp \tag{3.3}$$

a.e., where $\hat{n}$ is normal to the grain boundary (here we have used $\mathrm{Tr}(H) = 0$). We now use this characterization to obtain the following result concerning the set of recoverable strains of a polycrystal.

Proposition 3.1. *For any polycrystal,* $\dim(\overline{\mathcal{S}}) \leqslant 1$.

This result, along with the general properties of $\overline{\mathcal{S}}$ discussed earlier in Section 2 shows that $\overline{\mathcal{S}}$ is either $\{0\}$ or equal to the segment of a line centered at the origin. Further, it implies that any polycrystal with sufficient symmetry is necessarily rigid. Recall that $\overline{\mathcal{S}}$ has square symmetry (invariance under four-fold rotations). If the texture possess any additional symmetry (e.g., invariance under three-fold rotations, as we shall see in the next section), then it follows from this result that the polycrystal is necessarily rigid.

Bhattacharya & Kohn (1997, Thm. 5.3, pg.163) used the translation method to prove this result for strain fields in $L^2(\Omega, M^{2\times 2}_{\mathrm{sym}})$. Here we use duality in the context of $L^\infty(\Omega, M^{2\times 2}_{\mathrm{sym}})$.

Proof. For any polycrystal, we prove that $\bar{\epsilon}, \bar{\epsilon}' \in \overline{\mathcal{S}}$ only if $\bar{\epsilon} \parallel \bar{\epsilon}'$. The basic idea is to take any strain field associated with the average strain $\bar{\epsilon}$ and construct a test stress field for the dual variational principle (2.3) for $\bar{\epsilon}' \nparallel \bar{\epsilon}$.

If $\overline{\mathcal{S}} = \{0\}$, the result follows trivially. So let $0 \neq \bar{\epsilon} \in \overline{\mathcal{S}}$. Then, there exist $s, w \in L^\infty(\Omega, \mathbb{R})$ such that in a grain oriented at an angle θ, the displacement gradient H is of the form (3.1) and satisfies (3.2). Further, the jump in H satisfies $(3.3)_1$ almost everywhere along the grain boundaries. Finally,

$$\langle s(x,y)\hat{\epsilon}_{2\theta(x,y)}\rangle = \bar{\epsilon}. \tag{3.4}$$

Consider the field which in each grain is given by

$$\sigma(x,y) = w(x,y)I + \sqrt{2}s(x,y)\hat{\epsilon}_{2\theta(x,y)+\frac{\pi}{2}}. \tag{3.5}$$

Observe that this is a test field in the dual variational principle since it is divergence free: in each grain, (c.f. (3.2)),

$$\operatorname{div}(\sigma(x,y)) = \nabla w(x,y) - \left(\begin{smallmatrix} -\sin 2\theta & \cos 2\theta \\ \cos 2\theta & \sin 2\theta \end{smallmatrix}\right) \nabla s(x,y) = 0,$$

and satisfies $(3.3)_2$ a.e. along the grain boundaries:

$$\begin{aligned}
[\![\sigma(x,y)]\!] &= \frac{1}{\sqrt{2}}[\![w(x,y)I + \sqrt{2}s(x,y)\hat{\epsilon}_{2\theta(x,y)+\frac{\pi}{2}}]\!] \\
&= \frac{1}{\sqrt{2}}[\![\sqrt{2}s(x,y)\hat{\epsilon}_{2\theta(x,y)} + w(x,y)\left(\begin{smallmatrix} 0 & 1 \\ -1 & 0 \end{smallmatrix}\right)]\!]\left(\begin{smallmatrix} 0 & 1 \\ -1 & 0 \end{smallmatrix}\right) \\
&= \frac{1}{\sqrt{2}}[\![H(x,y)]\!]\left(\begin{smallmatrix} 0 & 1 \\ -1 & 0 \end{smallmatrix}\right) \\
&\parallel (\hat{n}^{\perp}(x,y) \otimes \hat{n}(x,y))\left(\begin{smallmatrix} 0 & 1 \\ -1 & 0 \end{smallmatrix}\right) \\
&= \hat{n}^{\perp}(x,y) \otimes \hat{n}^{\perp}(x,y)
\end{aligned}$$

where we have used $\hat{\epsilon}_{2\theta(x,y)+\frac{\pi}{2}} = \hat{\epsilon}_{2\theta(x,y)}\left(\begin{smallmatrix} 0 & 1 \\ -1 & 0 \end{smallmatrix}\right)$ and $(3.3)_1$. Further, using (3.4),

$$\begin{aligned}
\langle\sigma(x,y)\rangle &= \frac{1}{\sqrt{2}}\langle w(x,y)\rangle I + \langle s(x,y)\hat{\epsilon}_{2\theta(x,y)+\frac{\pi}{2}}\rangle \\
&= \frac{1}{\sqrt{2}}\langle w(x,y)\rangle I + \langle s(x,y)\hat{\epsilon}_{2\theta(x,y)}\rangle\left(\begin{smallmatrix} 0 & 1 \\ -1 & 0 \end{smallmatrix}\right) \\
&= \frac{1}{\sqrt{2}}\langle w(x,y)\rangle I + \bar{\epsilon}\left(\begin{smallmatrix} 0 & 1 \\ -1 & 0 \end{smallmatrix}\right).
\end{aligned} \tag{3.6}$$

Finally, note that $\sigma(x,y)\cdot\hat{\epsilon}_{2\theta(x,y)} = 0$. Now let $\bar{\epsilon}'$ be such that $\operatorname{Tr}(\bar{\epsilon}') = 0$. Using the field σ describe above in the dual variational principle, (2.3), and by recalling the dual energy (2.4), we conclude that

$$\begin{aligned}
\overline{W}(\bar{\epsilon}') &\geqslant \langle\sigma(x,y)\rangle\cdot\bar{\epsilon}' - \langle|\sigma(x,y)\cdot\hat{\epsilon}_{2\theta(x,y)}|\rangle \\
&= \langle\sigma(x,y)\rangle\cdot\bar{\epsilon}' \\
&= \langle w(x,y)\rangle I\cdot\bar{\epsilon}' + (\bar{\epsilon}'\left(\begin{smallmatrix} 0 & 1 \\ -1 & 0 \end{smallmatrix}\right))\cdot\bar{\epsilon} \\
&= (\bar{\epsilon}'\left(\begin{smallmatrix} 0 & 1 \\ -1 & 0 \end{smallmatrix}\right))\cdot\bar{\epsilon} \\
&> 0,
\end{aligned}$$

(by changing the sign of σ if necessary) except when $\bar{\epsilon}' \parallel \bar{\epsilon}$. Thus

$$0 \neq \bar{\epsilon} \in \overline{\mathcal{S}} \quad \Longrightarrow \quad \overline{\mathcal{S}} \subset \operatorname{Span}\{\bar{\epsilon}\} \quad \Longrightarrow \quad \dim(\overline{\mathcal{S}}) = 1. \qquad \square$$

We present another proof that does not use the dual variational principle, and is closer in spirit to Bhattacharya & Kohn (1997).

Proof. This is a proof by contradition. Assume that $\dim(\overline{\mathcal{S}}) = 2$ for some polycrystal. Then, recalling that $\overline{\mathcal{S}}$ is balanced and convex, it follows that there exists

$\bar{\epsilon} \neq 0$ such that $\bar{\epsilon} \in \overline{\mathcal{S}}$ and $R_{\frac{\pi}{4}}^T \bar{\epsilon} R_{\frac{\pi}{4}} = \bar{\epsilon} \left(\begin{smallmatrix} 0 & 1 \\ -1 & 0 \end{smallmatrix}\right) \in \overline{\mathcal{S}}$. Since $\bar{\epsilon} \in \overline{\mathcal{S}}$, we conclude by the arguments in the proof above that there exist $s, w \in L^\infty(\Omega, \mathbb{R})$ such that $\sigma \in L^\infty(\Omega, M^{2\times 2}_{\text{sym}})$ given by

$$\sigma(x,y) = w(x,y)I + \sqrt{2}s(x,y)\hat{\epsilon}_{2\theta(x,y)+\frac{\pi}{2}} \tag{3.5}$$

is divergence free and satisfies

$$\langle \sigma(x,y) \rangle = \langle w(x,y) \rangle I + \bar{\epsilon} \left(\begin{smallmatrix} 0 & 1 \\ -1 & 0 \end{smallmatrix}\right). \tag{3.6}$$

Since $\bar{\epsilon} \left(\begin{smallmatrix} 0 & 1 \\ -1 & 0 \end{smallmatrix}\right) \in \overline{\mathcal{S}}$, there exist $s', w' \in L^\infty(\Omega, \mathbb{R})$ such that $H \in L^\infty(\Omega, M^{2\times 2})$ given by

$$H(x,y) = \sqrt{2}s'(x,y)\hat{\epsilon}_{2\theta(x,y)} + w'(x,y) \left(\begin{smallmatrix} 0 & 1 \\ -1 & 0 \end{smallmatrix}\right) \tag{3.7}$$

is curl-free and satisfies

$$\langle H(x,y) \rangle = \bar{\epsilon} \left(\begin{smallmatrix} 0 & 1 \\ -1 & 0 \end{smallmatrix}\right) + \langle w'(x,y) \rangle \left(\begin{smallmatrix} 0 & 1 \\ -1 & 0 \end{smallmatrix}\right). \tag{3.8}$$

Thus, using (3.6) and (3.8),

$$|\bar{\epsilon}|^2 = (\bar{\epsilon} \left(\begin{smallmatrix} 0 & 1 \\ -1 & 0 \end{smallmatrix}\right)) \cdot (\bar{\epsilon} \left(\begin{smallmatrix} 0 & 1 \\ -1 & 0 \end{smallmatrix}\right)) = \langle \sigma(x,y) \rangle \cdot \langle H(x,y) \rangle.$$

Since σ is divergence free and H is curl free, one can integrate by parts (or use the div-curl lemma) to show that the right-hand side above which is a product of averages is in fact equal to the average of products. So,

$$\begin{aligned} |\bar{\epsilon}|^2 &= \langle \sigma(x,y) \cdot H(x,y) \rangle \\ &= \left\langle \left(w(x,y)I + \sqrt{2}s(x,y)\hat{\epsilon}_{2\theta(x,y)+\frac{\pi}{2}} \right) \cdot \left(\sqrt{2}s'(x,y)\hat{\epsilon}_{2\theta(x,y)} + w'(x,y) \left(\begin{smallmatrix} 0 & 1 \\ -1 & 0 \end{smallmatrix}\right) \right) \right\rangle \\ &= 0 \end{aligned}$$

by recalling (3.5) and (3.7). Thus $\bar{\epsilon} = 0$, which is a contradiction. □

4. Examples of rigid polycrystals

We describe examples of rigid polycrystals (i.e., those with $\overline{\mathcal{S}} = \{0\}$) in this section.

Example 4.1 (Hexagonal microstructures). The polycrystals shown in figures 1(a) and 1(b) are rigid. By inspection, the texture of these polycrystals is invariant under three-fold rotations. Therefore it follows from Proposition 3.1 that $\overline{\mathcal{S}} = \{0\}$. Figure 1(c) shows three stress fields for the polycrystal shown in figure 1(b). Any two of these suffice to independently show that the polycrystal is rigid.

We now show that even a polycrystal with square symmetry can be rigid.

Example 4.2 (Rigid checkerboard). The polycrystal shown in figure 2(a) is rigid.

Proof. Since we already know that $\overline{\mathcal{S}}$ is contained in the subspace of trace-free tensors, we only need to show that $\overline{W}(\bar{\epsilon}) > 0$ for each non-zero, trace-free $\bar{\epsilon}$.

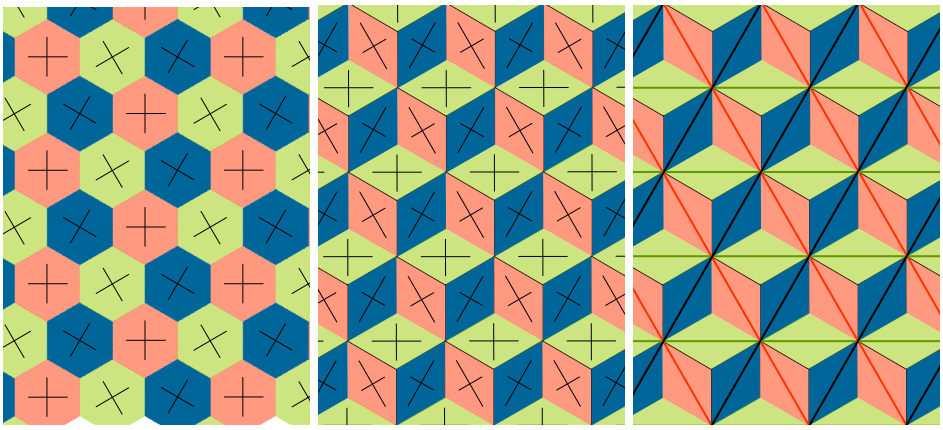

(a) (b) (c)

Figure 1. (a),(b) Polycrystals with 120° symmetry. The directions of the characteristics in each grain is shown. (c) Three independent dual fields for the polycrystal shown in (b).

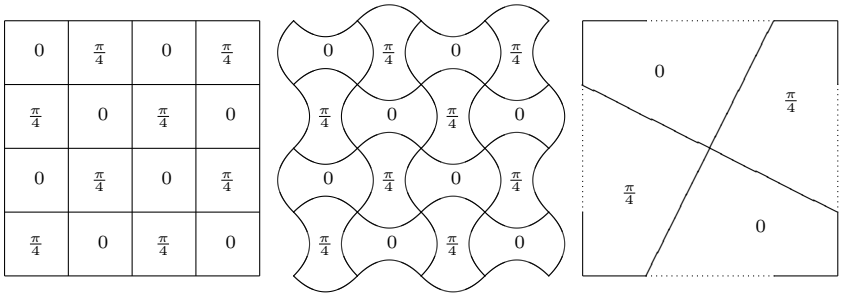

(a) Rigid checkerboard. (b) A variant of (a). (c) A variant of (a).

Figure 2. Three rigid polycrystals.

Consider a stress field σ concentrated on the diagonal line shown in figure 3(a) and taking the value $\left(\begin{smallmatrix}1\\1\end{smallmatrix}\right)\otimes\left(\begin{smallmatrix}1\\1\end{smallmatrix}\right)=\left(\begin{smallmatrix}1&1\\1&1\end{smallmatrix}\right)$. Note that this field is divergence free, has average $\frac{1}{2}\left(\begin{smallmatrix}1&1\\1&1\end{smallmatrix}\right)$, is supported in the grains oriented at 0, and has zero dual energy (c.f. (2.4)). Thus from (2.3), $\overline{W}(\bar{\epsilon})\geqslant\langle\sigma\rangle\cdot\bar{\epsilon}$ which — changing the sign of σ if necessary — is positive for each non-zero, trace-free $\bar{\epsilon}$ except when $\bar{\epsilon}\parallel\left(\begin{smallmatrix}1&0\\0&-1\end{smallmatrix}\right)$.

To dispose this remaining case when $\bar{\epsilon}\parallel\left(\begin{smallmatrix}1&0\\0&-1\end{smallmatrix}\right)$, consider a family σ_θ of stress fields, parameterized by $\theta\in(0,\frac{\pi}{4})$, concentrated on the lines shown in figure 3(a) and taking the value

$$\begin{cases}\left(\begin{smallmatrix}0\\1\end{smallmatrix}\right)\otimes\left(\begin{smallmatrix}0\\1\end{smallmatrix}\right) & \text{on the vertical line}\\ \frac{1}{2\sin\theta}\ \hat{n}(\theta)\otimes\hat{n}(\theta) & \text{on the lines inclined at } \theta\\ \frac{1}{2\sin\theta}\ \hat{n}(-\theta)\otimes\hat{n}(-\theta) & \text{on the lines inclined at } -\theta\end{cases}$$

Note that the field is divergence free and is supported within the grains oriented at $\frac{\pi}{4}$. Since each vertical line segment has length $1-\tan\theta$, and each inclined line

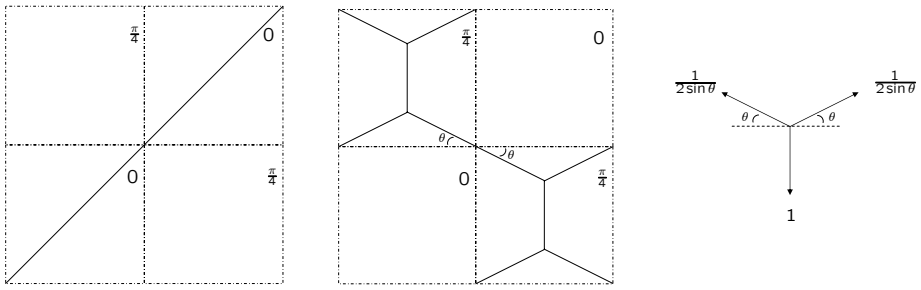

(a) (b)

Figure 3. Dual fields for the rigid checkerboard and a free body diagram showing force equilibrium.

segment has length $\frac{1}{2\sin\theta}$, the average value of this field is

$$\begin{aligned}\langle\sigma_\theta\rangle &= \frac{1}{2}(1-\tan\theta)\left(\begin{smallmatrix}0\\1\end{smallmatrix}\right)\otimes\left(\begin{smallmatrix}0\\1\end{smallmatrix}\right) + \frac{1}{4\sin^2\theta}\hat{n}(\theta)\otimes\hat{n}(\theta) + \frac{1}{4\sin^2\theta}\hat{n}(-\theta)\otimes\hat{n}(-\theta)\\ &= \frac{1}{2}(1-\tan\theta)\left(\begin{smallmatrix}0&0\\0&1\end{smallmatrix}\right) + \frac{1}{4\sin^2\theta}\left(\left(\begin{smallmatrix}\cos^2\theta & -\cos\theta\sin\theta\\ -\cos\theta\sin\theta & \sin^2\theta\end{smallmatrix}\right) + \left(\begin{smallmatrix}\cos^2\theta & \cos\theta\sin\theta\\ \cos\theta\sin\theta & \sin^2\theta\end{smallmatrix}\right)\right)\\ &= \frac{1}{2}(1-\tan\theta)\left(\begin{smallmatrix}0&0\\0&1\end{smallmatrix}\right) + \frac{1}{2\sin^2\theta}\left(\begin{smallmatrix}\cos^2\theta & 0\\ 0 & \sin^2\theta\end{smallmatrix}\right)\\ &= \frac{1}{2}\left(\begin{smallmatrix}\frac{1}{\tan^2\theta} & 0\\ 0 & 2-\tan\theta\end{smallmatrix}\right),\end{aligned}$$

and average dual energy is

$$\langle\widehat{W}^\star(R^T(x)\sigma_\theta R(x))\rangle = \frac{\sqrt{2}}{4\sin^2\theta}\,|-\cos\theta\sin\theta| + \frac{\sqrt{2}}{4\sin^2\theta}\,|\cos\theta\sin\theta| = \frac{1}{\sqrt{2}\tan\theta}.$$

Note that the ratio

$$\frac{\langle\widehat{W}^\star(R^T(x)\sigma_\theta R(x))\rangle}{\langle\sigma_\theta\rangle\cdot\left(\begin{smallmatrix}1&0\\0&-1\end{smallmatrix}\right)} = \frac{2\sqrt{2}\tan\theta}{\frac{1}{\tan^2\theta}-2+\tan\theta} \to 0^+ \text{ as } \theta\to 0.$$

Thus for every $0\neq\bar{\epsilon}\parallel\left(\begin{smallmatrix}1&0\\0&-1\end{smallmatrix}\right)$ with $|\bar{\epsilon}|$ sufficiently small, there exists θ such that $\overline{W}(\bar{\epsilon})\geqslant\langle\sigma_\theta\rangle\cdot\bar{\epsilon}-\langle\widehat{W}^\star(R^T(x)\sigma_\theta R(x))\rangle>0$. □

Remark 4.3. Variations of this example are possible. For instance, the above proof shows that the polycrystal shown in figure 2(b) is rigid. Moreover, for this polycrystal a stress field simpler than that shown in figure 3(b) exists, namely one concentrated on a vertical or horizontal line contained in the grains oriented at $\frac{\pi}{4}$ and passing through the corners where the grains meet. A similar construction shows that the polycrystal in 2(c) is rigid.

5. Examples of flexible polycrystals

Example 5.1 (Flexible strip). The polycrystal shown in figure 4(a) is flexible. For the grain oriented at $\frac{\pi}{4}$, the associated characteristics are horizontal and vertical. Since a family of horizontal characteristics percolates through this grain, it is

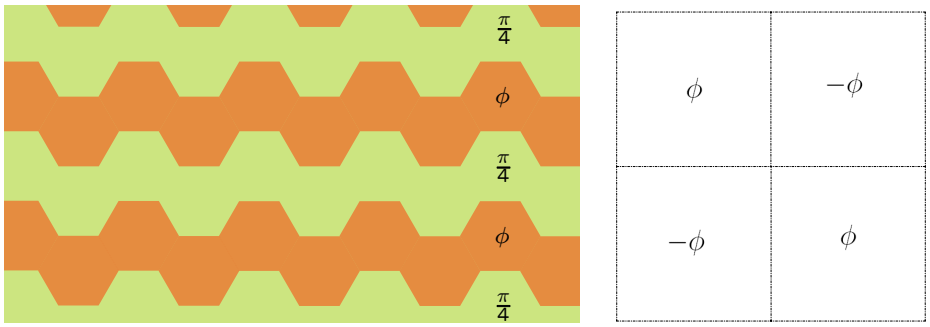

(a) (b)

Figure 4. Two flexible polycrystals. For the checkerboard, $\phi \in (0, \frac{\pi}{4})$.

possible to construct non-trivial piecewise constant strain fields that are non-zero on (horizontal) strips in this grain and zero otherwise.

Example 5.2 (Flexible checkerboard). For the polycrystal shown in figure 4(b),

$$\overline{\mathcal{S}} = \{s \left(\begin{smallmatrix} 0 & 1 \\ 1 & 0 \end{smallmatrix}\right) \mid s \in \mathbb{R}, |s| \leqslant \tan\phi\}\,.$$

Proof. Step 1: $\overline{\mathcal{S}} \supset \{s \left(\begin{smallmatrix} 0 & 1 \\ 1 & 0 \end{smallmatrix}\right) \mid s \in \mathbb{R}, |s| \leqslant \tan\phi\}$.
Consider the piecewise constant displacement gradient field shown in figure 5(b) (the corresponding deformation is shown in 5(a)). Here $\hat{n}_- = \hat{n}(-\phi - \frac{\pi}{4})$, $\hat{n}_-^\perp = \hat{n}(-\phi + \frac{\pi}{4})$, $\hat{n}_+ = \hat{n}(\phi - \frac{\pi}{4})$ and $\hat{n}_+^\perp = \hat{n}(\phi + \frac{\pi}{4})$. Note that

$$\hat{n}_- \otimes \hat{n}_-^\perp - \hat{n}_-^\perp \otimes \hat{n}_- = \left(\begin{smallmatrix} 0 & 1 \\ -1 & 0 \end{smallmatrix}\right), \qquad \hat{n}_+ \otimes \hat{n}_+^\perp - \hat{n}_+^\perp \otimes n_+ = \left(\begin{smallmatrix} 0 & 1 \\ -1 & 0 \end{smallmatrix}\right),$$
$$\hat{n}_- \otimes \hat{n}_-^\perp + \hat{n}_-^\perp \otimes \hat{n}_- = \sqrt{2}\epsilon_{-2\phi}, \qquad \hat{n}_+ \otimes \hat{n}_+^\perp + \hat{n}_+^\perp \otimes \hat{n}_+ = \sqrt{2}\epsilon_{2\phi}.$$

With this it is easy to see that all jump conditions are satisfied and that the strain field lies within the zero set of each grain. Indeed, from (2.2) within the inner square in each grain, the strain field lies at the boundary of the zero set of that grain. Let each grain of the polycrystal be a square whose side is of length 1. The area of the inner square is $\frac{\sec^2\theta}{2}$. Thus the average strain in the polycrystal is

$$\frac{\sec^2\theta}{4}\left(\sqrt{2}\epsilon_{2\phi} - \sqrt{2}\epsilon_{-2\phi}\right) = \tan\phi \left(\begin{smallmatrix} 0 & 1 \\ 1 & 0 \end{smallmatrix}\right).$$

This completes step 1. To complete the proof, we prove the reverse inclusion.
Step 2: $\overline{\mathcal{S}} \subset \{s \left(\begin{smallmatrix} 0 & 1 \\ 1 & 0 \end{smallmatrix}\right) \mid s \in \mathbb{R}, |s| \leqslant \tan\phi\}$.
Consider a stress field σ concentrated on the lines shown in figure 6(a) (see also figure 6(b)). On each line segment the value of the field is proportional to $\hat{t} \otimes \hat{t}$ where $\hat{t}$ is tangent to the line; the magnitude of the value of the field on each line segment is marked in figure 6(a).

Note that

$$\widehat{AB} = \begin{pmatrix} \cos(\frac{\pi}{4} - \phi) \\ -\sin(\frac{\pi}{4} - \phi) \end{pmatrix}, \qquad \widehat{BC} = \begin{pmatrix} -\cos(\phi + \frac{\pi}{4}) \\ -\sin(\phi + \frac{\pi}{4}) \end{pmatrix}, \qquad \widehat{CA} = \begin{pmatrix} -\cos(\frac{\pi}{2} - \phi) \\ \sin(\frac{\pi}{2} - \phi) \end{pmatrix},$$

$$\widehat{A'B'} = \begin{pmatrix} -\cos(\phi + \frac{\pi}{4}) \\ \sin(\phi + \frac{\pi}{4}) \end{pmatrix}, \qquad \widehat{B'C'} = \begin{pmatrix} \cos(\frac{\pi}{4} - \phi) \\ \sin(\frac{\pi}{4} - \phi) \end{pmatrix}, \qquad \widehat{C'A'} = \begin{pmatrix} -\cos(\frac{\pi}{2} - \phi) \\ -\sin(\frac{\pi}{2} - \phi) \end{pmatrix}.$$

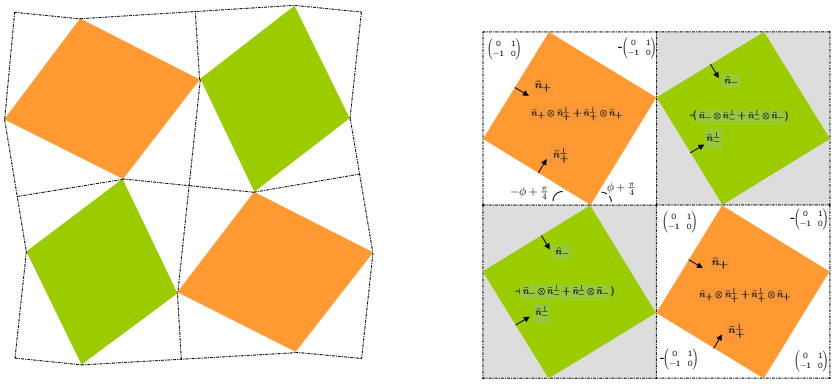

(a) (b)

Figure 5. (a) A deformation and (b) the corresponding displacement gradient field for the flexible checkerboard.

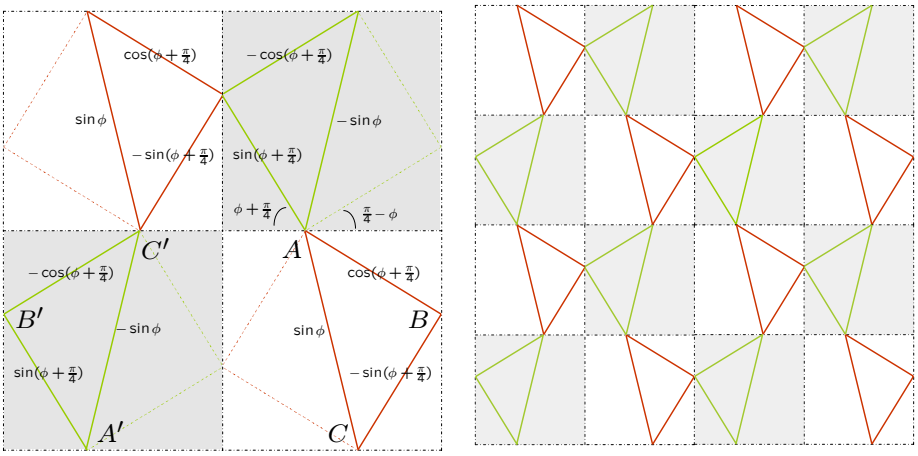

(a) A dual field for the flexible checkerboard. (b) The same dual field as in (a) with more grains shown.

Figure 6.

To verify that this field is divergence free, it is sufficient to verify equilibrium at the points marked A/A', B/B' and C/C' in figure 6(a) (see figure 7):

$$
\begin{aligned}
-\sin\phi\ \widehat{A'C'} + \sin(\phi+\frac{\pi}{4})\ \widehat{A'B'} + \sin\phi\ \widehat{AC} + \cos(\phi+\frac{\pi}{4})\ \widehat{AB} &= 0,\\
-\cos(\phi+\frac{\pi}{4})\ \widehat{B'C'} + \cos(\phi+\frac{\pi}{4})\ \widehat{BA} - \sin(\phi+\frac{\pi}{4})\ \widehat{BC} + \sin(\phi+\frac{\pi}{4})\ \widehat{B'A'} &= 0,\\
-\sin(\phi+\frac{\pi}{4})\ \widehat{CB} + \sin\phi\ \widehat{CA} - \cos(\phi+\frac{\pi}{4})\ \widehat{C'B'} - \sin\phi\ \widehat{C'A'} &= 0,
\end{aligned}
$$

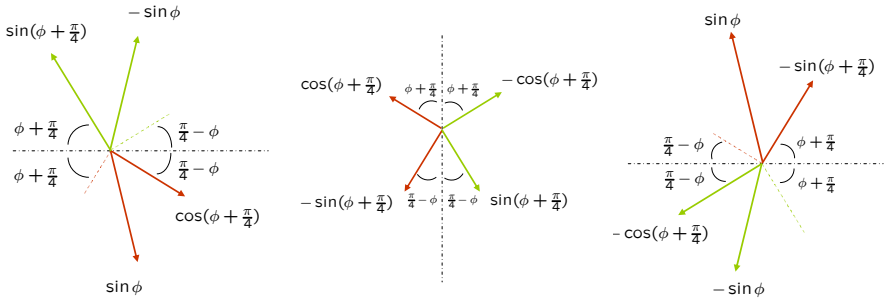

(a) Equilibrium at A/A'. (b) Equilibrium at B/B'. (c) Equilibrium at C/C'.

Figure 7. Free body diagrams for dual field shown in figure 6(a).

respectively. This is easily verified.

Let L be the length of a side of the inner square (shown partially in dotted lines in figure 6(a)). Then

$$\begin{aligned}\frac{2}{L}\langle\sigma\rangle = \sqrt{2}\sin\phi\left(\begin{pmatrix}\cos(\phi+\frac{\pi}{2})\\ \sin(\phi+\frac{\pi}{2})\end{pmatrix}\otimes\begin{pmatrix}\cos(\phi+\frac{\pi}{2})\\ \sin(\phi+\frac{\pi}{2})\end{pmatrix}-\begin{pmatrix}\cos(\frac{\pi}{2}-\phi)\\ \sin(\frac{\pi}{2}-\phi)\end{pmatrix}\otimes\begin{pmatrix}\cos(\frac{\pi}{2}-\phi)\\ \sin(\frac{\pi}{2}-\phi)\end{pmatrix}\right)\\ -\sin(\phi+\frac{\pi}{4})\left(\begin{pmatrix}\cos(\phi+\frac{\pi}{4})\\ \sin(\phi+\frac{\pi}{4})\end{pmatrix}\otimes\begin{pmatrix}\cos(\phi+\frac{\pi}{4})\\ \sin(\phi+\frac{\pi}{4})\end{pmatrix}-\begin{pmatrix}-\cos(\phi+\frac{\pi}{4})\\ \sin(\phi+\frac{\pi}{4})\end{pmatrix}\otimes\begin{pmatrix}-\cos(\phi+\frac{\pi}{4})\\ \sin(\phi+\frac{\pi}{4})\end{pmatrix}\right)\\ +\cos(\phi+\frac{\pi}{4})\left(\begin{pmatrix}-\cos(\frac{\pi}{4}-\phi)\\ \sin(\frac{\pi}{4}-\phi)\end{pmatrix}\otimes\begin{pmatrix}-\cos(\frac{\pi}{4}-\phi)\\ \sin(\frac{\pi}{4}-\phi)\end{pmatrix}-\begin{pmatrix}\cos(\frac{\pi}{4}-\phi)\\ \sin(\frac{\pi}{4}-\phi)\end{pmatrix}\otimes\begin{pmatrix}\cos(\frac{\pi}{4}-\phi)\\ \sin(\frac{\pi}{4}-\phi)\end{pmatrix}\right)\\ =\sqrt{2}\cos\phi\begin{pmatrix}0&1\\1&0\end{pmatrix}.\end{aligned}$$

The average dual energy $\langle\widehat{W}^\star(R^T(x)\sigma R(x))\rangle$ is given by

$$\begin{aligned}2\langle\widehat{W}^\star(R^T(x)\sigma R(x))\rangle = (\sqrt{2}L)\sqrt{2}\left|\sin\phi\begin{pmatrix}\cos(\phi+\frac{\pi}{2})\\ \sin(\phi+\frac{\pi}{2})\end{pmatrix}\otimes\begin{pmatrix}\cos(\phi+\frac{\pi}{2})\\ \sin(\phi+\frac{\pi}{2})\end{pmatrix}\cdot\hat{\epsilon}_{2\phi}\right|\\ +(\sqrt{2}L)\sqrt{2}\left|\sin\phi\begin{pmatrix}\cos(\frac{\pi}{2}-\phi)\\ \sin(\frac{\pi}{2}-\phi)\end{pmatrix}\otimes\begin{pmatrix}\cos(\frac{\pi}{2}-\phi)\\ \sin(\frac{\pi}{2}-\phi)\end{pmatrix}\cdot\hat{\epsilon}_{-2\phi}\right|\\ =2\sqrt{2}L\sin\phi.\end{aligned}$$

Thus for any $\bar{\epsilon}=\lambda\begin{pmatrix}0&1\\1&0\end{pmatrix}$, changing the sign of σ if necessary,

$$\overline{W}(\bar{\epsilon})=\langle\sigma\rangle\cdot\bar{\epsilon}-\widehat{W}^\star(R^T(x)\sigma R(x))=(|\lambda|\cos\phi-\sin\phi)\sqrt{2}L,$$

which is positive whenever $|\lambda|>\tan\phi$. □

We now provide another, more direct, proof that shows that any non-trivial strain-field in this checkerboard is necessarily of the type constructed in step 1.

Proof. Consider any zero-energy displacement gradient field H in the flexible checkerboard. From §3(a), on the characteristics numbered as shown in figure 8,

$$H = \begin{cases} h_n^+ \ \hat{n}(\phi - \frac{\pi}{4}) \otimes \hat{n}(\phi + \frac{\pi}{4}) & |n|\text{: odd} \\ h_n^+ \ \hat{n}(\phi + \frac{\pi}{4}) \otimes \hat{n}(\phi - \frac{\pi}{4}) & |n|\text{: even} \end{cases}$$

in the grains oriented at ϕ, and

$$H = \begin{cases} h_n^- \ \hat{n}(-\phi + \frac{\pi}{4}) \otimes \hat{n}(-\phi - \frac{\pi}{4}) & |n|\text{: odd} \\ h_n^+ \ \hat{n}(-\phi - \frac{\pi}{4}) \otimes \hat{n}(-\phi + \frac{\pi}{4}) & |n|\text{: even} \end{cases}$$

in the grains oriented at $-\phi$. Here $h_n^+, h_n^- \in \mathbb{R}$. Imposing displacement compatibility at the points where characteristics meet we obtain

$$\begin{pmatrix} h_{n+1}^- \\ h_{n+1}^+ \\ h_{-(n+1)}^- \\ h_{-(n+1)}^+ \end{pmatrix} = \begin{cases} \frac{1}{2} \begin{pmatrix} \tan^2(\phi+\frac{\pi}{4})-1 & \sec^2(\phi+\frac{\pi}{4}) & 0 & 0 \\ \sec^2(\phi+\frac{\pi}{4}) & \tan^2(\phi+\frac{\pi}{4})-1 & 0 & 0 \\ 0 & 0 & \tan^2(\phi+\frac{\pi}{4})-1 & \sec^2(\phi+\frac{\pi}{4}) \\ 0 & 0 & \sec^2(\phi+\frac{\pi}{4}) & \tan^2(\phi+\frac{\pi}{4})-1 \end{pmatrix} \begin{pmatrix} h_n^- \\ h_n^+ \\ h_{-n}^- \\ h_{-n}^+ \end{pmatrix} & n > 0, \text{ odd} \\ \frac{1}{2} \begin{pmatrix} \tan^2(\phi+\frac{\pi}{4})-1 & 0 & 0 & \sec^2(\phi+\frac{\pi}{4}) \\ 0 & \tan^2(\phi+\frac{\pi}{4})-1 & \sec^2(\phi+\frac{\pi}{4}) & 0 \\ 0 & \sec^2(\phi+\frac{\pi}{4}) & \tan^2(\phi+\frac{\pi}{4})-1 & 0 \\ \sec^2(\phi+\frac{\pi}{4}) & 0 & 0 & \tan^2(\phi+\frac{\pi}{4})-1 \end{pmatrix} \begin{pmatrix} h_n^- \\ h_n^+ \\ h_{-n}^- \\ h_{-n}^+ \end{pmatrix} & n > 0, \text{ even} \end{cases}$$

Each of the matrices above has eigenvalues -1 and $\tan^2(\phi+\frac{\pi}{4}) > 1$. The eigenspaces corresponding to -1 are

$$\begin{cases} \text{Span}\left\{(1,-1,0,0)^T, (0,0,1,-1)^T\right\} & n\text{: odd} \\ \text{Span}\left\{(1,0,0,-1)^T, (0,1,-1,0)^T\right\} & n\text{: even.} \end{cases}$$

These relations are recursive, alternating between the odd and even cases. Therefore, unless the vector $(h_1^-, h_1^+, h_{-1}^-, h_{-1}^+)^T$ lies in the intersection of eigenspaces corresponding to -1 of both matrices, either $h_n^\pm$ or $h_{-n}^\pm$ will grow unbounded (as some integer power of $\tan^2(\phi + \frac{\pi}{4})$). Such a strain field does not remain in the zero set $\widehat{\mathcal{S}}$. On the other hand, if $(h_1^-, h_1^+, h_{-1}^-, h_{-1}^+)^T$ lies in the intersection of eigenspaces corresponding to -1 of both matrices, $(h_n^-, h_n^+, h_{-n}^-, h_{-n}^+)^T$ also lies in this space for all n. This implies that the only strain field that remains in the zero set $\widehat{\mathcal{S}}$ a.e. is one that satisfies $(h_n^-, h_n^+, h_{-n}^-, h_{-n}^+)^T = \lambda(-1)^n(1,-1,1,-1)^T$ for some $|\lambda| \leqslant 1$. It is easy to verify that the displacement gradient field that results from the choice $(h_n^-, h_n^+, h_{-n}^-, h_{-n}^+)^T = (-1)^n(1,-1,1,-1)^T$ is the field constructed in step 1 of the earlier proof. □

Between steps 1 and 2 above we implicitly used proposition 3.1 to deduce that $\overline{\mathcal{S}} \subset \text{Span}\{\left(\begin{smallmatrix} 0 & 1 \\ 1 & 0 \end{smallmatrix}\right)\}$. It is possible to also show this by constructing stress fields.

Consider the stress field σ concentrated on the spiralling lines shown in figure 9(a) (see also figure 9(b)). In each grain, the spiral consists of 'arms' of straight line

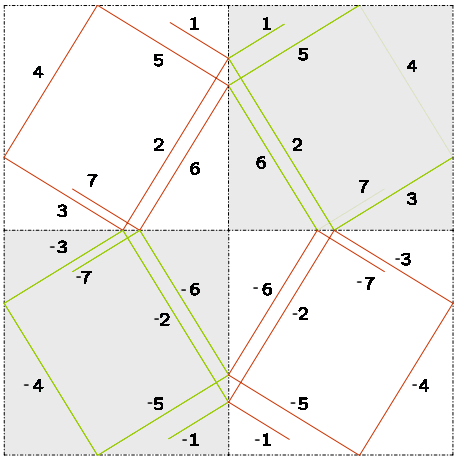

Figure 8. A segment of an arbitrary zero-energy displacement gradient field in the flexible checkerboard.

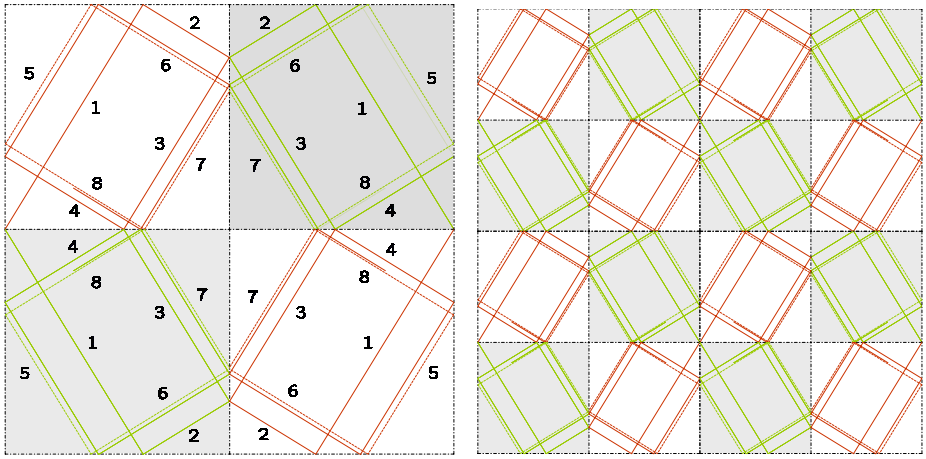

(a) A dual field for the flexible checkerboard. (b) The same dual field as in (a) with more grains shown.

Figure 9.

segments which are numbered as shown. The spiral converges to the square shown in dashed lines. This is the same square as in figure 5(b).

The value of the stress on the n^{th} arm of the spiral is given by

$$\sigma = \begin{cases} \cot^n(\phi + \frac{\pi}{4})\ \hat{n}(\phi + \frac{\pi}{4}) \otimes \hat{n}(\phi + \frac{\pi}{4}) & n\text{: odd} \\ \cot^n(\phi + \frac{\pi}{4})\ \hat{n}(\phi - \frac{\pi}{4}) \otimes \hat{n}(\phi - \frac{\pi}{4}) & n\text{: even} \end{cases}$$

in the grains oriented at ϕ, and by

$$\sigma = \begin{cases} \cot^n(\phi + \frac{\pi}{4})\ \hat{n}(-\phi + \frac{\pi}{4}) \otimes \hat{n}(-\phi + \frac{\pi}{4}) & n\text{: odd} \\ \cot^n(\phi + \frac{\pi}{4})\ \hat{n}(-\phi - \frac{\pi}{4}) \otimes \hat{n}(-\phi - \frac{\pi}{4}) & n\text{: even} \end{cases}$$

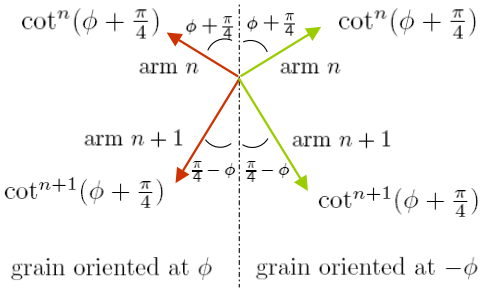

Figure 10. A free body diagram showing force equilibrium at the point where arms n and $n+1$ meet for the stress field shown in figure 9(a).

in the grains oriented at $-\phi$. It is clear that this field is divergence free within each grain; it is easy to check using figure 10 that it is also divergence free at the grain boundaries.

The lengths of the arms satisfy the recurrence relation

$$\begin{aligned} L_1 \cos(\frac{\pi}{4}-\phi) &= 1 \\ L_n \cos(\phi+\frac{\pi}{4}) + L_{n+1}\cos(\frac{\pi}{4}-\phi) &= 1 \end{aligned}$$

which can be solved to give

$$L_n = \frac{\sec\phi}{\sqrt{2}}\left(1-\left(-\cot(\phi+\frac{\pi}{4})\right)^n\right).$$

Averaging over both grains, the average value of σ in the n^{th} arm is

$$\begin{cases} \frac{1}{2}\cot^n(\phi+\frac{\pi}{4}) \begin{pmatrix} \cos^2(\phi+\frac{\pi}{4}) & 0 \\ 0 & \sin^2(\phi+\frac{\pi}{4}) \end{pmatrix} & n\text{:odd}, \\ \frac{1}{2}\cot^n(\phi+\frac{\pi}{4}) \begin{pmatrix} \cos^2(\frac{\pi}{4}-\phi) & 0 \\ 0 & \sin^2(\frac{\pi}{4}-\phi) \end{pmatrix} & n\text{:even}. \end{cases}$$

Thus the net average value of the stress is parallel to

$$\begin{aligned} &\begin{pmatrix} \cos^2(\phi+\frac{\pi}{4}) & 0 \\ 0 & \sin^2(\phi+\frac{\pi}{4}) \end{pmatrix} \sum_{n\text{:odd}} \left(\cot^n(\phi+\frac{\pi}{4})(1-(-\cot(\phi+\frac{\pi}{4}))^n)\right) \\ &\quad + \begin{pmatrix} \cos^2(\frac{\pi}{4}-\phi) & 0 \\ 0 & \sin^2(\frac{\pi}{4}-\phi) \end{pmatrix} \sum_{n\text{:odd}} \left(\cot^n(\phi+\frac{\pi}{4})(1-(-\cot(\phi+\frac{\pi}{4}))^n)\right) \end{aligned}$$

which is parallel to $\begin{pmatrix} \cos(\phi+\frac{\pi}{4}) & 0 \\ 0 & \sin(\phi+\frac{\pi}{4}) \end{pmatrix}$. Thus from (2.3), $\overline{W}(\bar{\epsilon}) \geqslant \langle\sigma\rangle\cdot\bar{\epsilon}$ which — changing the sign of σ if necessary — is positive except when $\bar{\epsilon} \parallel \left(\begin{smallmatrix} 0 & 1 \\ 1 & 0 \end{smallmatrix}\right)$.

Finally, note that by superposing the stress field considered in the preceeding proof with a diagonally translated copy of itself we obtain another stress field which is shown in figures 11(a) and 11(b). This resulting stress field is more (globally) symmetric than the preceeding stress field. Other variations are also possible.

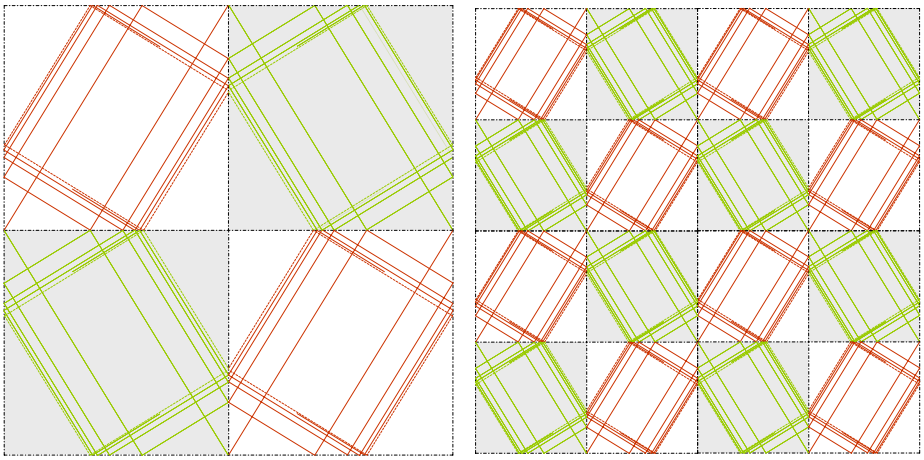

(a) A dual field for the flexible checkerboard. (b) The same dual field as in (a) with more grains shown.

Figure 11.

Remark 5.3. The flexible checkerboard shows that the zero-set of a polycrystal can depend discontinuously on microstructure. As $\phi \to 0$, $\overline{\mathcal{S}} \to \{0\}$. However, when $\phi = 0$, the checkerboard reduces to a single crystal and $\overline{\mathcal{S}} = \left\{ s \left(\begin{smallmatrix} 1 & 0 \\ 0 & -1 \end{smallmatrix}\right) \mid s \in \mathbb{R}, |s| \leqslant 1 \right\}$!

Scalar examples presented in Bhattacharya & Kohn (1997, §4) lead to the conjecture that a polycrystal is flexible only when strips supporting gradients traverse or 'percolate' through it. The flexible checkerboard shows that the situation is more complex in the context of strain and percolation can be through isolated points.

Variations of the flexible checkerboard are possible; for example, the polycrystal shown in figure 12(a).

Example 5.4. Consider a displacement gradient field consisting of three square regions of constant displacement gradient arranged around a triangle (rather than four around a rhombus as in the flexible checkerboard). This pattern can be periodically extended; see figure 12(b). If one picks a periodic texture with three-fold symmetry that is consistent with this displacement gradient, then the polycrystal with that texture is rigid by proposition 3.1. Yet it can support strain fields that are not identically zero.

It would be interesting to study small perturbations of this texture, and ask whether the polycrystal would become flexible, but unfortunately our tools are currently inadequate to do so.

6. Remarks on Plasticity

We briefly discuss application of these ideas to plasticity. Consider an incompressible rigid-perfectly plastic material (in two-dimensions) with two slip systems, $\left(\begin{smallmatrix} 1 & 0 \\ 0 & -1 \end{smallmatrix}\right)$ with yield strength 1 and $\left(\begin{smallmatrix} 0 & 1 \\ 1 & 0 \end{smallmatrix}\right)$ with yield strength M. If $M \gg 1$, the crystal can slip easily on one system, $\left(\begin{smallmatrix} 1 & 0 \\ 0 & -1 \end{smallmatrix}\right)$, while it is almost constrained in the other. Such a crystal is said to be *deficient*. An interesting and important question is the plastic

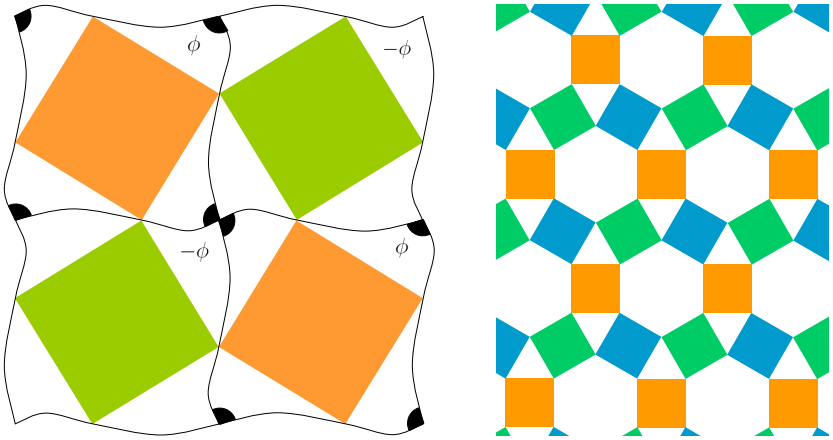

(a) A variant of the flexible checkerboard that supports the deformation gradient shown in figure 5(b). The regions shown in black are inclusions of arbitrary orientation.

(b) A displacement gradient field (constant in each of the coloured squares) that generalizes that of the flexible polycrystal. The texture of the polycrystal is not shown.

Figure 12. Variants of the flexible checkerboard.

behavior of a polycrystal made of such a material. This has motivated recent work in the scalar setting following Kohn & Little (1998).

By scaling the stress by $1/M$ and letting $M \to \infty$, we obtain a problem very similar to what we have studied above. Now the material has zero yield stress in the $\left(\begin{smallmatrix} 1 & 0 \\ 0 & -1 \end{smallmatrix}\right)$ system and unit yield strength in the $\left(\begin{smallmatrix} 0 & 1 \\ 1 & 0 \end{smallmatrix}\right)$ system. We describe this by introducing an yield set,

$$\mathcal{Y} = \left\{ \sigma \in M^{2\times 2}_{\text{sym}} \mid \sigma \cdot \left(\begin{smallmatrix} 1 & 0 \\ 0 & -1 \end{smallmatrix}\right) = 0,\ \left|\sigma \cdot \left(\begin{smallmatrix} 0 & 1 \\ 1 & 0 \end{smallmatrix}\right)\right| \leq 1 \right\},$$

a stress potential

$$W^\star(\sigma) = \begin{cases} 0 & \sigma \in \mathcal{Y} \\ \infty & \text{otherwise,} \end{cases}$$

and complimentary strain energy,

$$W(\epsilon) = \begin{cases} \left| \left(\begin{smallmatrix} 1 & 0 \\ 0 & -1 \end{smallmatrix}\right) \cdot \epsilon \right| & \operatorname{Tr} \epsilon = 0 \\ \infty & \text{otherwise.} \end{cases}$$

Note that $\mathcal{Y}$ is two-dimensional and unbounded in the $\left(\begin{smallmatrix} 1 & 0 \\ 0 & 1 \end{smallmatrix}\right)$ direction. The effective behavior of a polycrystal is again described through variational principles

$$\begin{aligned} \overline{W}^\star(\bar{\sigma}) &:= \inf_{\substack{\sigma(x) \in \mathcal{S}^{\text{p}}_{\text{ad}} \\ \langle \sigma(x) \rangle = \bar{\sigma}}} \fint_\Omega W^\star(R^T(x)\sigma(x)R(x))\ \mathrm{d}x \\ &= \sup_{\epsilon \in \mathcal{U}^{\text{p}}_{\text{ad}}} \fint_\Omega \bar{\sigma} \cdot \epsilon - W(R^T(x)\epsilon(x)R(x))\ \mathrm{d}x. \end{aligned}$$

where

$$\mathcal{S}^{\mathrm{p}}_{\mathrm{ad}} := \left\{\sigma \in L^{\infty}_{\mathrm{per}}(\Omega, M^{2\times 2}_{\mathrm{sym}}) \mid \mathrm{div}(\sigma) = 0\right\},$$
$$\mathcal{U}^{\mathrm{p}}_{\mathrm{ad}} := \left\{u \in L^{\infty}(\Omega, \mathbb{R}^2) \mid \epsilon(u) \in M^{1}_{\mathrm{per}}(\Omega, M^{2\times 2}_{\mathrm{sym}})\right\}.$$

Note that the stress-fields are bounded and the strains are measures here. $\overline{W}^{\star}$ vanishes on $\overline{\mathcal{Y}}$ and is infinite otherwise. The effective yield set $\overline{\mathcal{Y}}$ is unbounded in the $\left(\begin{smallmatrix}1 & 0\\ 0 & 1\end{smallmatrix}\right)$ direction, and is convex, balanced and contains the origin. The issue is to understand the nature of the set $\overline{\mathcal{Y}}_0 := \overline{\mathcal{Y}} \cap \{\sigma \mid \mathrm{Tr}\,\sigma = 0\}$. We say that the polycrystal is *degenerate*, *deficient* or *rigid* depending on whether the dimension of $\overline{\mathcal{Y}}_0$ is 0, 1 or 2, respectively.

It is also easy to verify that the stress field with zero stress potential and the strain and deformation gradient fields with zero strain energy are exactly as described in §3(a). We can use this to prove the following analog of proposition 3.1.

Proposition 6.1. *For any polycrystal,* $\dim(\overline{\mathcal{Y}}_0) \leqslant 1$.

Thus, a polycrystal of this material is never rigid. Further, polycrystals with sufficient symmetry are always degenerate.

Turning now to the examples, it is easy to show that polycrystals with hexagonal grains (example 4.1; figures 1(a) and 1(b)) are degenerate as is the checkerboard we had describe earlier as rigid (example 4.2, remark 4.3; figure 2). In contrast, the polycrystals in examples 5.1 and 5.2 (figure 4) are deficient. In working out these examples it is useful to note that shear strain fields $\hat{t}\otimes\hat{t}^{\perp} + \hat{t}^{\perp}\otimes\hat{t}$ can be supported on lines with tangent $\hat{t}$.

Results for finite but large M will be considered in future work.

Acknowledgement. This work draws from IVC's doctoral thesis at the California Institute of Technology. We are grateful to Pierre Suquet and Gal deBotton for useful discussions. We acknowledge the partial financial support of US Army Research Office through the MURI grant DAAD19-01-1-0517 and the US Office of Naval Research through the grant N00014-01-1-0937.

References

Bhattacharya, K. 2003. *Microstructure of martensite. Why it forms and how it gives rise to the shape-memory effect.* Oxford University Press.

Bhattacharya, K. & Kohn, R. V. 1997. Elastic energy minimization and the recoverable strains of polycrystalline shape-memory materials. *Arch. Rational Mech. Anal.*, **139**, 99–180.

Bhattacharya, K., Kohn, R. V., & Kozlov, S. 1999. Some examples of nonlinear homogenization involving nearly degenerate energies. *Proc. R. Soc. Lond. A*, **455**, 567–583.

Bhattacharya, K. & Suquet, P. 2004. A model problem for recoverable strains in polycrystals (draft).

Chenchiah, I. 2004. *Energy-minimizing microstructures in multiphase elastic solids.* PhD thesis, California Institute of Technology.

Demengel, F. & Suquet, P. 1986. On locking materials. *Acta Appl. Math.*, **6**, 185–211.

DeSimone, A. & James, R.D. 2002. A constrained theory of magnetoelasticity. *J. Mech. and Phys. Solids*, **50**, 283-320.

Garroni, A. & Kohn, R. V. 2003. Some three-dimensional problems related to dielectric breakdown and polycrystal plasticity. *Proc. R. Soc. Lond. A*, **459**, 2613–2625.

Goldsztein, G. H. 2001. Rigid perfectly plastic two-dimensional polycrystals. *Proc. R. Soc. Lond. A*, **457**, 2789–2798.

Goldsztein, G. H. 2003. Two-dimensional rigid polycrystals whose grains have one ductile direction. *Proc. R. Soc. Lond. A*, **459**, 1949–1968.

Drucker, D. C. 1966. The continuum theory of plasticity on the macroscale and the microscale. *J. Mat.*, **1**, 873–910.

Drucker, D. C., Prager W. & Greenberg, H.J. 1952. Extended limit design theorems for continuous media. *Quart. Appl. Math.*, **9**, 381-389.

Hill, R. 1950. *The mathematical theory of plasticity.* Oxford University Press.

Kocks, U.F., Tomé, C.N. & Wenk, H.R. 1998. *Texture and anisotropy: preferred orientations in polycrystal and their effect on material properties.* Cambridge University Press.

Kohn, R. V. & Little, T. D. 1998. Some model problems of polycrystal plasticity with deficient basic crystals. *SIAM J. Appl. Math.*, **59**(1), 172–197.

Prager, W. 1957. On ideal locking materials. *Trans. Soc. Rheology*, **1**(1), 169–175.